

Response to Referee #2: Joshua Brinkerhoff

Authors' responses to reviewer comments after major revision appear in purple text.

We would like to express our sincere gratitude to the referee for their valuable time and effort in reviewing our paper, as well as for their insightful suggestions.

Authors' responses to reviewer comments appear in blue text. Line numbers referenced in the authors' responses refer to the revised document. Figures with Arabic numerals (e.g., Figure 10) correspond to the revised manuscript; figures with Roman numerals (e.g., Figure iv) only appear in response to the reviewer's comments.

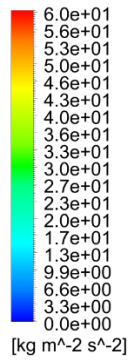
1. Overall, I found the paper to be rather lengthy in its description of the AD method and associated momentum theory, which is not novel.

Thank you for your feedback on the length of the paper's description regarding the AD method and associated momentum theory. We have carefully considered your comment and made revisions to reduce the extent of this section while still ensuring clarity and comprehension. In this respect, general descriptions of Momentum and Blade element theories were eliminated from sections 3.1 and 3.2. Moreover, primary equations in these theories, i.e., equations 1, 2, 13, 14, and 15, and their descriptions were removed from the sections. Nevertheless, the secondary equations resulting from the substitution of various variables in these equations were retained to convey the fundamental principles of the BEM theory.

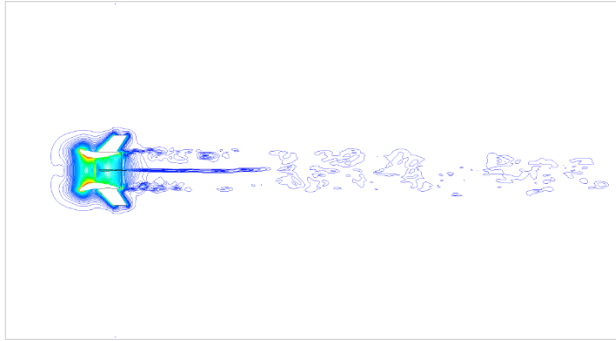
2. I expected to see the sensitivity of the computational domain size, which was not provided and my intuition suggests is small, especially the upstream distance between the inlet and the balloon turbine.

To complete the determination of the domain dimensions, it was solved separately by different domain sizes and observing the variable flow gradients at the boundaries. The computational domain was chosen as the minimum size that exhibited zero gradients at the boundaries. Figure i illustrates the pressure gradients for $U_{\text{ref}} = 7 \text{ m s}^{-1}$ and $\theta_{\text{tilt}} = 0^\circ, 5^\circ$ and 10° on a symmetry plane of the balloon in the finalized domain. The pressure contours provide an evident indication that there is no pressure gradient present at the boundary of the domain with the determined dimensions.

Pressure.Gradient
Contour 1

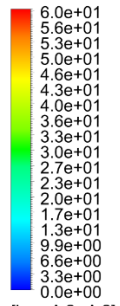


[kg m⁻² s⁻²]

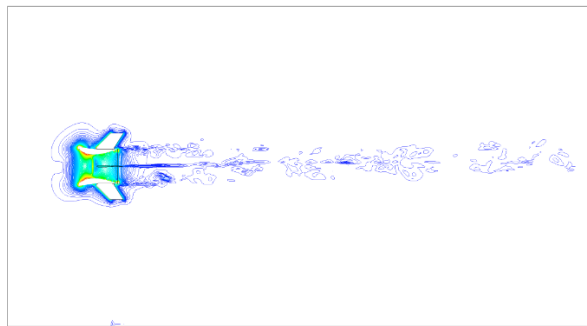


(a)

Pressure.Gradient
Contour 2



[kg m⁻² s⁻²]



(b)

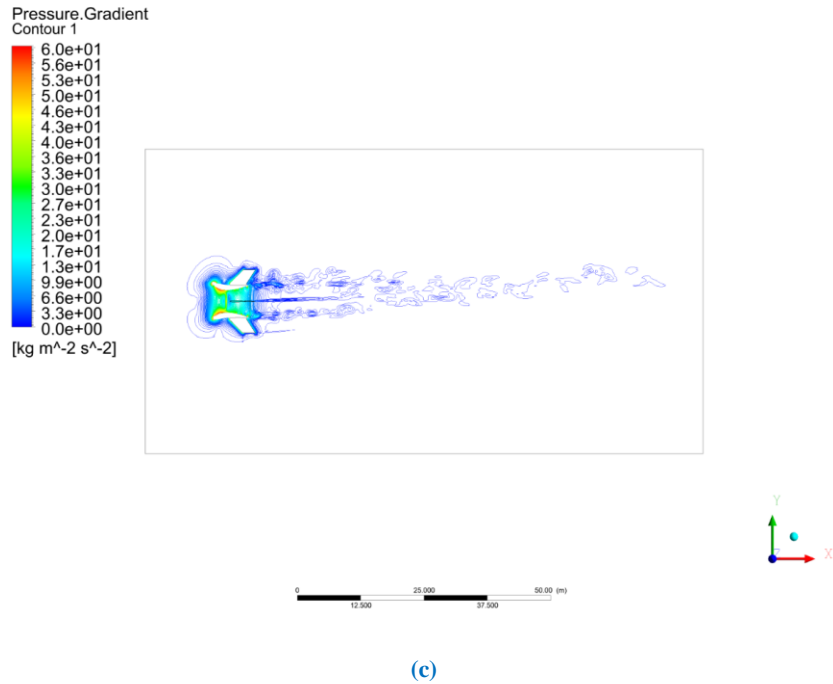
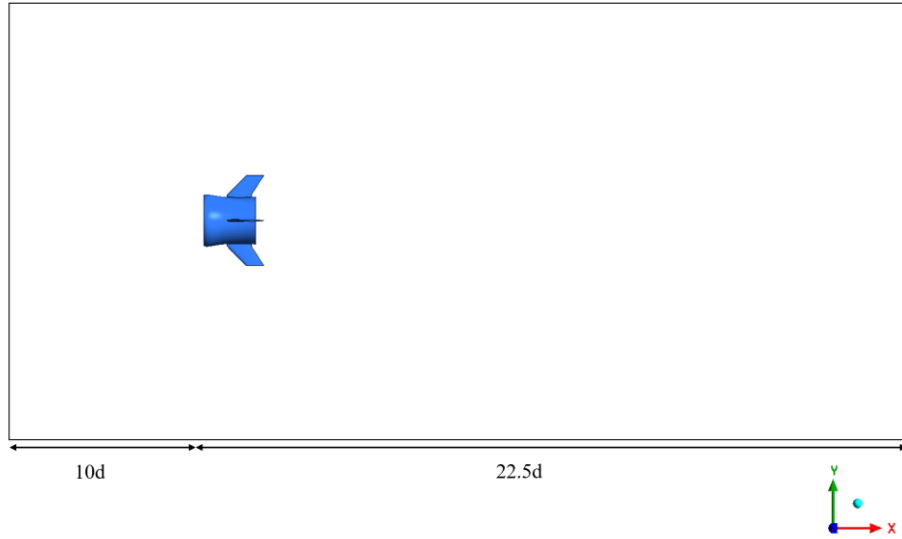
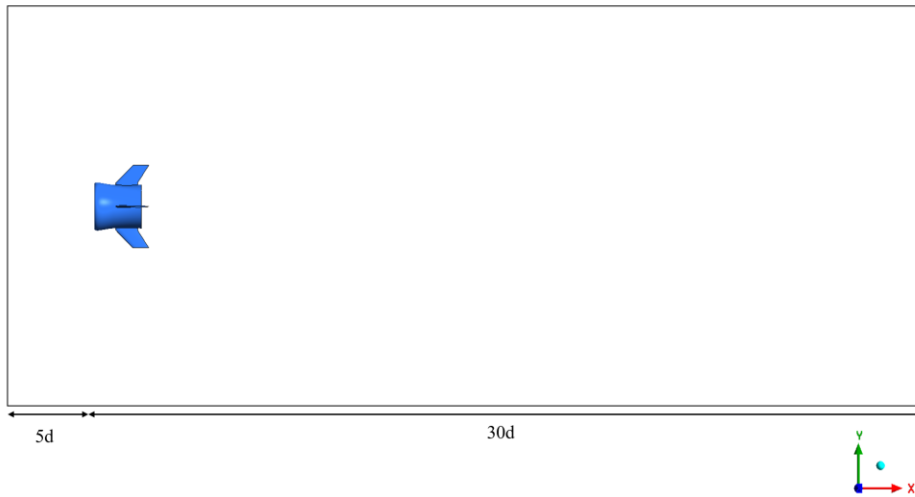


Figure i. Pressure gradient contour for $U_{ref} = 7 \text{ m s}^{-1}$ and (a) $\theta_{tilt} = 0^\circ$, (b) $\theta_{tilt} = 5^\circ$ (c) $\theta_{tilt} = 10^\circ$ on the symmetry plane of the balloon ($z=0$).

In response to the referee's query regarding the sensitivity of the computational domain size, we would like to provide additional information to further support the appropriateness of the domain size chosen in our study. In our initial response, we explained that the domain dimensions were carefully determined by evaluating flow gradients at the boundaries, to select a size that ensured zero gradients. While this method was valid, we employed sensitivity analysis of wake characteristics in relation to domain size here to further support the reliability of our approach. In light of this, we have conducted a follow-up study wherein we created two different computational domains: one with an extended upstream length (from 5d to 10d) and another with an extended downstream length (from 22.5d to 30d) as shown in figure ii relative to the turbine position, beyond the original domain utilized in the research. We increased the number of nodes in the upstream distance by a factor of 2 for the extended upstream domain and by 1.3 times (equal to the length increment ratio) for the extended downstream domain to ensure consistent spatial resolution in all cases, while only considering changes in the computational domain size on the results.



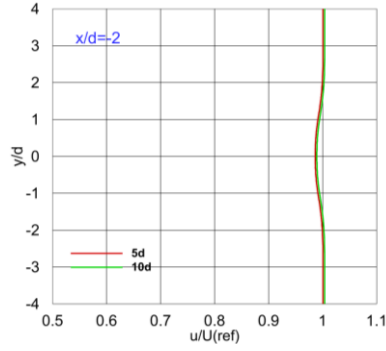
(a)



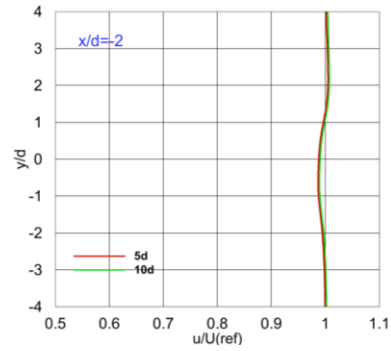
(b)

Figure ii. Computational domain size for (a) extended upstream length and (b) extended downstream length.

With these new computational domains, we applied the same simulation settings and boundary conditions as described in Section 4 of the paper to conduct simulations for the cases where $U_{\text{ref}} = 7 \text{ m s}^{-1}$ and $\theta_{\text{tilt}} = 0^\circ$ and 10° . Figure iii showcases the simulation results employing an extended upstream length, illustrating vertical profiles of the time-averaged normalized x-velocity at $x/d = -2$, within the range of $-4 < y/d < 4$ at $z = 0$. Additionally, figure iv presents the outcomes of the simulation utilizing an extended downstream length, displaying vertical profiles of the time-averaged normalized x-velocity at $x/d = 5$ and 14 , within the range of $-4 < y/d < 4$ at $z = 0$.

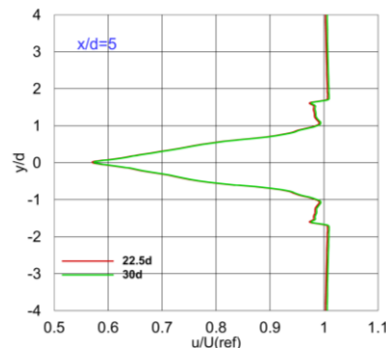


(a)

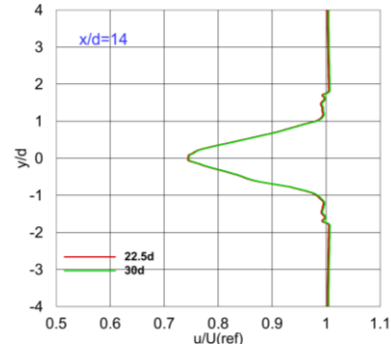


(b)

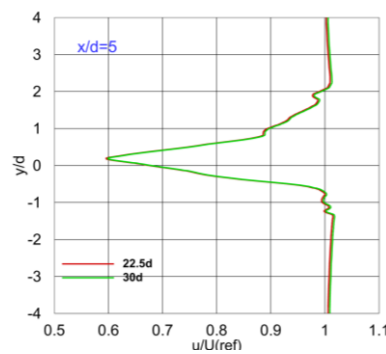
Figure iii. Comparison of vertical profiles of the time-averaged normalized x-velocity for different upstream lengths for $U_{ref}=7 \text{ m s}^{-1}$ and $-4 < y/d < 4$, and $z=0$ with $\theta_{tilt} =$ (a) 0° (b) 10° at $x/d = -2$.



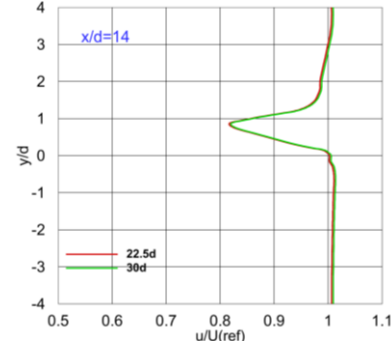
(a)



(b)



(c)



(d)

Figure iv. Comparison of vertical profiles of the time-averaged normalized x-velocity for different downstream lengths for $U_{ref}=7 \text{ m s}^{-1}$ and $-4 < y/d < 4$, and $z=0$ with $\theta_{tilt} = 0^\circ$ at (a) $x/d = 5$ (b) $x/d = 14$ and $\theta_{tilt} = 10^\circ$ at (c) $x/d = 5$ (d) $x/d = 14$.

According to figure iii, extending upstream lengths has been observed to have a relatively minor impact on the velocity profiles at various locations relative to the wind turbine position. This observation can be ascribed to the specific conditions governing our investigation. Notably, we considered our wind turbine situated at a high altitude where the atmosphere tends to be more stable because it is less influenced by surface heating and friction, which can lead to reduced turbulence and vertical mixing. The absence of significant boundary layer effects due to the high-altitude location of our wind turbine led to a longer upstream length less critical for capturing boundary layer-related phenomena. These specific environmental conditions enabled us to design our computational domain with a smaller upstream length than typically required for studying ground-based wind turbine wake behaviour, prioritizing computational efficiency while maintaining result accuracy.

Furthermore, as shown in figure iv, prolonging the downstream distances has shown only a marginal influence on the velocity profiles at different positions relative to the wind turbine's location. Our choice of downstream length was carefully considered in light of several critical factors. The selected downstream domain size was designed to encompass the essential characteristics of the wake, including wake recovery, turbulence decay, and gradual mixing with ambient air. This careful consideration of downstream length was paramount to accurately capturing the wake's behaviour and its impact on downstream flow. In summary, under these controlled conditions and with careful attention to factors critical to wake simulation, the impact of extending the domain size upstream and downstream remained minimal, providing robust support for the appropriateness of our chosen computational domain size.

3. Secondly, the analysis to ensure consistent spatial resolution relies on a RANS simulation for estimating the turbulence kinetic energy and dissipation rate for calculating the turbulence integral scale. The details of the RANS simulation are not provided. Moreover, why the RANS solution can be considered accurate is not justified.

The details of the RANS simulations and the reasons for choosing this model to calculate turbulence kinetic energy and dissipation rate are added in Line (257) of the manuscript as follows:

Line (257): The K-Omega SST model was employed in the precursor simulations, utilizing simulation setup and boundary conditions similar to those described in section 4 of the paper, duplicating the main model configuration. The K-Omega SST model accurately estimates turbulence kinetic energy and dissipation by employing a dual-equation formulation, which captures the interactions between these quantities more comprehensively. Additionally, its enhanced near-wall treatment improves accuracy in capturing boundary layer characteristics around the balloon surface, making it a reliable choice for precise calculations.

In response to the referee's inquiry regarding the accuracy and reliability of the RANS solutions used in our methodology for generating LES-friendly meshes, we appreciate the opportunity to provide a more detailed explanation and justification.

Verification and Validation: To ensure the accuracy of the RANS solutions leading to the generation of LES-friendly meshes, we undertook several measures:

1. **Comparison with Experimental Data:** In the case of smaller wind turbine where experimental data were available, our LES-friendly mesh generation approach was applied to simulate the wake behaviour of the turbine. The results derived from this approach exhibited a good level of agreement with the corresponding experimental data, providing persuasive evidence for the appropriateness of the mesh generated based on the RANS simulation results.
2. **Grid Independence:** We rigorously assessed the quality of the mesh generation algorithm by conducting grid independence studies for both the smaller turbine and balloon wind turbine simulations as described in response to questions 4 and 5 in this document. Our methodology consistently satisfied grid independence criteria, indicating the mesh's suitability and the reliability of the RANS solutions.
3. **Convergence Criterion:** Our simulations consistently met the convergence criterion of 1×10^{-4} for residuals across all cases. This demonstrates the stability and convergence of the RANS solutions, further affirming their accuracy.

In cases where experimental data were not available for the balloon wind turbine study, we acknowledge the limitation of direct experimental validation. However, we firmly believe that the combined evidence from the successful agreement with experimental data in a similar case, grid independence, and convergence criteria support the appropriateness and accuracy of the RANS solutions employed for LES-friendly mesh generation.

4. Thirdly, the grid independence assesses the pressure coefficient distribution along the balloon periphery, which is not convincing for assessing grid independence of the results. More convincing would be to demonstrate the grid independence of the wake recovery, separation zone size and strength, and other parameters that would be expected to be more sensitive to the grid.

Thank you for your valuable comment regarding the assessment of grid independence in our paper. We appreciate your suggestion and would like to address your concern. In our previous evaluation of grid independence, we focused on the pressure coefficient distribution along the balloon periphery. While this aspect provides some insights into the grid independence of aerodynamic loads on balloons, we acknowledge that it may not be the most convincing parameter for evaluating grid independence of the wake characteristics, which is the leading study concern. Therefore, to avoid excessive length in this section resulting from the inclusion of grid independence analysis for both parameters, we have opted to focus our analysis on the grid size effect, specifically on wake recovery. Consequently, we have made the necessary revisions in Line (272) in the manuscript as follows:

Line (272): To further assess the criterion, its grid independence was investigated. Accordingly, two coarser (G1) and finer (G3) meshes, summarized in Table 1, were generated. By employing these meshes in three simulations, a comparison was conducted on the vertical profiles of the time-averaged normalized x-velocity at three distinct downstream locations. All of the simulations were performed for $U_{\text{ref}} = 10 \text{ m s}^{-1}$ and $\theta_{\text{tilt}} = 0^\circ$ and the results are illustrated in Figure 10. According to Figure 10, using a coarser grid in the near wake leads to a lower prediction of velocity deficit. This is because as the grid size grows, the small-scale turbulence structures and vortices are not

accurately resolved. As a result, the flow tends to smooth out, and the turbulence effects are underestimated. This can lead to an underprediction of the velocity deficit in the near wake. However, the difference in average velocity at 3d downstream of the turbine between mesh G3 and G2 is about 1%, while this difference is around 4% for meshes G2 and G1. Moreover, the difference between velocity profiles for different grids decreases in further regions. Since the discrepancy between G2 and G1 mesh results is about one-fourth of the difference between G2 and G3, the mesh criterion in LES satisfies the wake recovery's mesh independence requirement.

Table 1
Mesh distribution in the computational domain for evaluating mesh criterion in LES.

| Grid number | G1 | G2 | G3 |
|---|-----------|------------|-------------|
| Nodes on edge N_{in} | 23 | 43 | 50 |
| Nodes on edge N_{wing} | 25 | 35 | 40 |
| Nodes on edge N_{out} | 25 | 30 | 40 |
| Nodes on edge N_u | 20 | 30 | 40 |
| Nodes on edge N_s | 74 | 86 | 95 |
| Nodes on edge N_d | 250 | 285 | 300 |
| Nodes on edge N_p | 140 | 196 | 236 |
| Nodes within the boundary layers N_{bl} | 35 | 35 | 35 |
| Total Number of nodes N_t | 4,972,096 | 10,756,364 | 15,4657,804 |

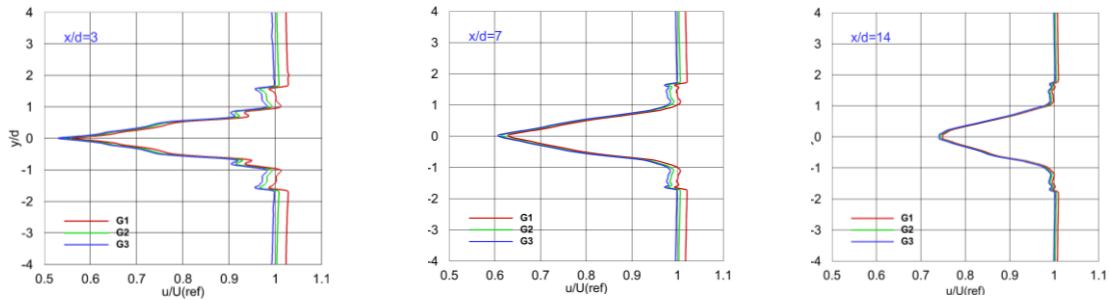


Figure 10. Vertical profiles of the time-averaged x-velocity at different locations downstream of the turbine.

5. Fourthly, the validation against experiment is not well documented--the authors do not comment on the spatial resolution of the validation study and whether it is consistent with the main study. The result is that the validation--which does show good agreement--does not convincingly demonstrate the accuracy of the main study results.

To clarify the spatial resolution of the validation study, we add the node distribution in the domain in Line (301) of the manuscript as follows:

Line (301): The cubic domain was discretized with 192, 32, and 42 nodes along the x and y axes.

Moreover, we added a section in Line (319) of the manuscript to evaluate the grid independence of the results of the validation study as below:

Line (319): To assess the grid independence of velocity profiles in the wake, the simulations were performed for a coarser and finer mesh. The number of nodes in the coarser and finer grids along

the x, y, and z directions was $120 \times 25 \times 30$ and $250 \times 50 \times 60$ respectively. Figure 14 shows the comparison of vertical profiles of the time-averaged streamwise velocity obtained from the experimental study and 3 different grids. According to Figure 14, decreasing the grid size has a minor effect on the velocity profiles within the wake, and the results obtained from the main grid demonstrate good consistency with experimental measurements.

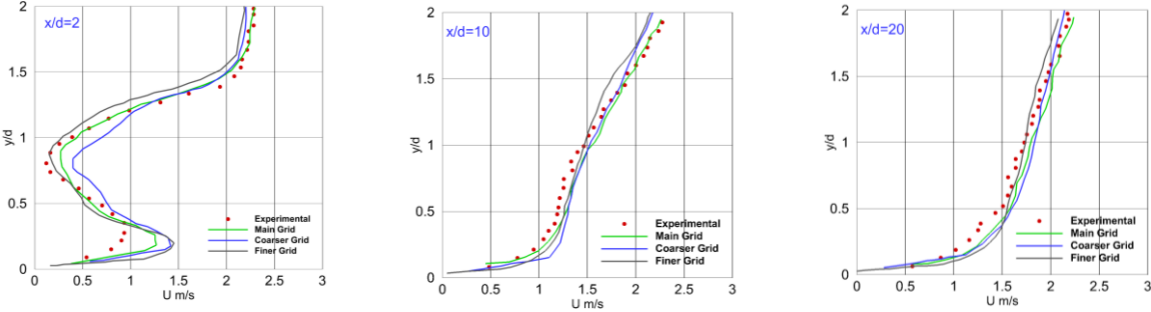


Figure 14. Comparison of vertical profiles of the time-averaged streamwise velocity U (m s^{-1}) obtained by the experiment and different grids.